ARTICLE NO. 78-829R

Wind-Tunnel Measurements of the Surface Pressure Distribution on a Spinning Magnus Rotor

Miles C. Miller*
Department of the Army, Aberdeen Proving Ground, Md.

The aerodynamic pressure distribution acting on the surface of a spinning four-vaned, cylindrical Magnus rotor in cross flow was experimentally obtained during a series of subsonic wind tunnel tests. A pressure tap located in the non-spinning inner portion of the wind tunnel model detected the surface pressures through a series of vent holes in the spinning outer portion of the model. The pressures were measured by means of a sliding seal arrangement. For the test condition used, $V = 100$ fps and $R_d = 277{,}000$, the autorotating (steady state) tip speed ratio of this Magnus rotor was 0.46, corresponding to a spin rate of 2050 rpm. Surface pressure distribution over the entire circumference of the spinning Magnus rotor are presented at 1 ms intervals. Resultant lift and drag coefficients computed by integrating the measured pressure distribution data reveal the cyclic nature of the lift and drag with time and their relative phase relations. Comparison of measured pressure distribution profiles with corresponding smoke flow data indicates the unsteady, periodic separated flowfield and illustrates the powerful tool provided by the pressure distribution toward interpreting and analyzing aerodynamic phenomena on spinning configurations having irregular external shapes.

Nomenclature

b = span of model
C_D = drag coefficient, $D/q_\infty S$
C_L = lift coefficient, $L/q_\infty S$
C_P = pressure coefficient, $\Delta P/q_\infty$
D = drag force
d = diameter of model
L = lift force
P = aerodynamic pressure on surface of model
P_∞ = freestream static pressure
q_∞ = dynamic pressure, $\rho_\infty V_\infty{}^2/2$
R_d = Reynolds number, $V_\infty d/\nu$
S = reference area, bd
t = time
V_∞ = freestream velocity
ΔP = pressure on surface of model referred to freestream static pressure, $P - P_\infty$
α = angle of attack
ρ_∞ = air density
ν = kinematic viscosity
ϕ = circumferential location on model at which pressure is being measured (angle between radial direction of pressure tap and freestream velocity)
Ψ = model rotational attitude (angle between flat external surface of driving vane and freestream velocity)
Ω = spin rate
$\hat{\omega}$ = tip speed ratio, $\omega d/2V$

Introduction

A MAGNUS rotor (autorotor) is an asymmetrically shaped body that, when placed in an airstream, will autorotate or spin, thereby producing large aerodynamic lift and drag forces. Magnus rotor configurations have been utilized for such diverse applications as self-dispersing submunitions,[1] aerodynamic decelerators,[2,3] and windmill blades.[4] The aerodynamic design of these items has been based primarily on the results of extensive parametric wind tunnel investigations. Further, these wind tunnel data have been limited to the static force and moment type which does not provide detailed insight into how these forces are generated.

Considerable effort has been expended to evolve a fundamental fluid dynamic theory which describes the aerodynamic forces and moment acting on a Magnus rotor.[5] As yet, a quantitative theory of this type does not exist. This is due in no small part to the presence of an unsteady periodic separated vortex flow. Knowledge of the aerodynamic pressure distribution acting over a spinning Magnus rotor could aid in evolving a theoretical fluid dynamic analysis. In addition, it would represent actual data with which theoretical results could be compared. This paper describes the experimental determination of the aerodynamic surface pressure distribution acting on a spinning Magnus rotor. These data were obtained during a subsonic wind tunnel test of a spinning cylindrical Magnus rotor in cross flow using a unique model design and instrumentation arrangement.

Model Description

The external configuration of the Magnus rotor wind tunnel model is illustrated in Fig. 1. The model consists of a right circular cylinder incorporating four full-span driving vanes. Circular plates are located at each end of the model to eliminate tip flow effects and consequent spanwise pressure gradients. This rotor configuration is representative of Magnus rotors in general and possesses typical aerodynamic characteristics.[6]

The internal arrangement of the model is presented in Fig. 2. The model includes a stationary (i.e., nonspinning) cylindrical core containing a pressure tap oriented radially outward at a fixed angle ϕ to the direction of the freestream velocity. The angle ϕ defines the circumferential location on the surface of the model at which the pressure is being measured. A thin-walled, cylindrical shell is located concentrically around the core and is attached to the core by means of bearings located at each end. The shell is free to rotate or spin about the core and represents the external surface of the spinning body.

Presented as Paper 78-829 at the AIAA 10th Aerodynamic Testing Conference, San Diego, Calif., April 19-21, 1978; submitted May 30, 1978; revision received May 29, 1979.

Index category: Jets, Wakes, and Viscid-Inviscid Flow Interactions.

*Project Engineer, Army Armament Research and Development Command. Member AIAA.

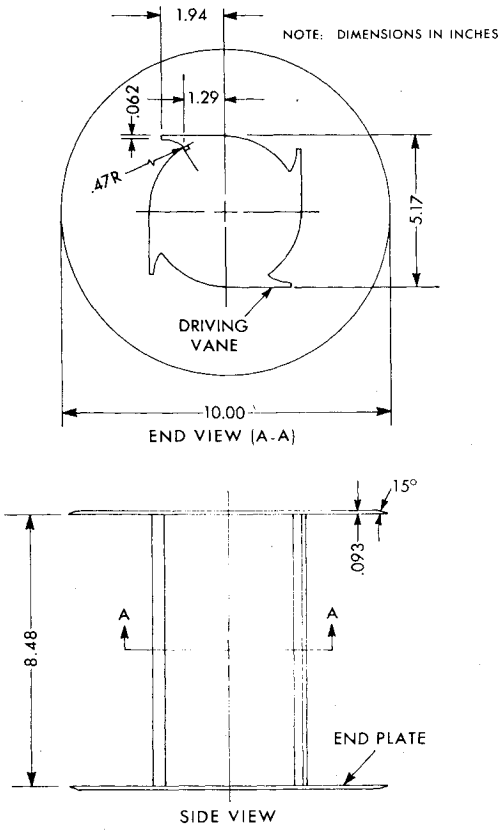

Fig. 1 External configuration of wind tunnel model.

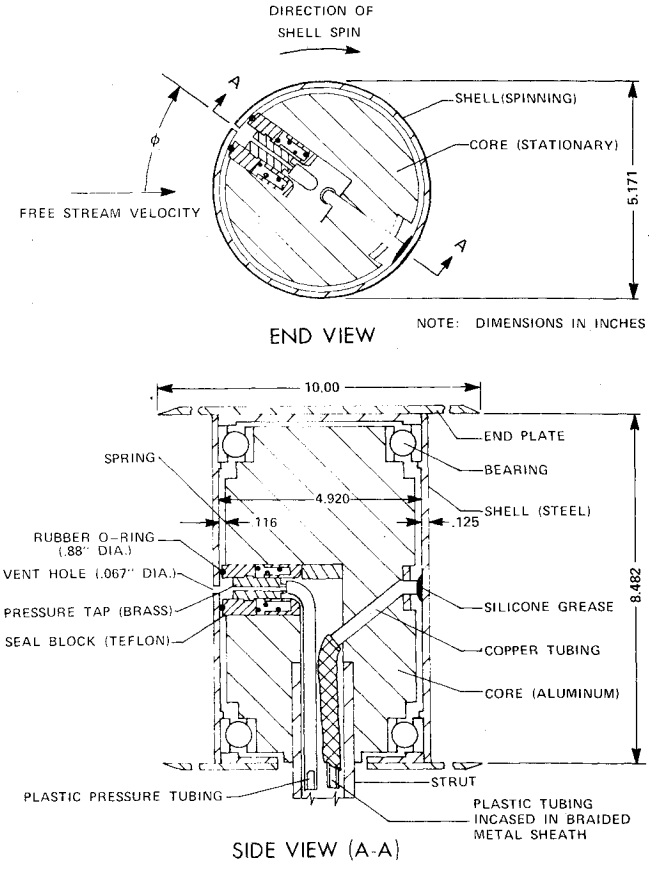

Fig. 2 Internal details of wind tunnel model.

A 0.069 in. diam vent hole is located through the shell at midspan such that it will line up with the face of the pressure tap once every revolution of the shell about the core. The gap between the face of the pressure tap and the inner surface of the shell is sealed in all directions (i.e., longitudinally and circumferentially) by means of a circular rubber "O" ring seal located around the face of the pressure tap assembly. Small coil springs in the pressure tap assembly press the "O" ring against the inner surface of the shell to affect a tight sliding seal. The cylindrical cavity created within this seal will be open to the pressure acting on the outside surface of the shell when the vent hole is aligned with the tap. When the shell vent hole rotates past this aligned position, the sliding seal will cause the cavity to retain this pressure. The pressure is transmitted by plastic tubing routed through the model core and the model attachment strut to a pressure transducer and associated instrumentation equipment located outside of the tunnel.

The vent hole is only aligned with the cavity for a very short time every revolution. Several revolutions of the spinning shell are required in order to have the pressure in the cavity reach a condition of equilibrium with a constant pressure equal to that acting on the outside surface of the shell. Since the pressure is constant, the transducer response time is not critical.

Pressure measurements at various circumferential locations on the surface of the spinning body can be obtained by positioning the core and the attached tap at different attitudes ϕ to the air flow. This is accomplished by rotating the core about its longitudinal axis to a particular angle and holding it there sufficiently long to obtain the pressure measurement.

The basic testing method was utilized previously in wind tunnel tests of a spinning smooth cylinder model in cross flow.[7,8] The model used in these earlier tests has been modified to the Magnus rotor configuration by simply adding the four driving vanes and additional vent holes. One change made to the model interior from that of the earlier feasibility tests is the addition of a self-contained lubrication feature. A section of copper tubing is located within the model core and oriented radially outward 180 deg to the pressure tap. This tubing is attached to plastic tubing enclosed in a braided material metal sheath which is routed down the model strut to a grease gun mechanism located outside the tunnel. The plastic tubing is filled with silicone grease prior to the test. A single stroke of the grease gun handle provides a slow but steady flow of silicone grease onto the inner surface of the spinning shell surface thereby providing continuous lubrication to the seal during the test. Also, a soft rubber "O" ring having a circular cross section is used in the Magnus rotor tests as opposed to the harder rubber "quad-ring" used during the tests with the smooth cylinder. This change in "O" ring configuration allows the seal spring force to be decreased to 8 lb thereby reducing the spin motor power requirements.

It should be noted that for the earlier tests with the smooth cylinder, difficulties were experienced with the seal spring and seal lubrication mechanisms. This resulted in frequent stoppages to adjust the spring and manually lubricate the seal—an event which occurred several times during a circumferential survey. Several hours were required to complete a single circumferential survey, with consequent changes in Reynolds number occurring during a particular test. Although the pressure data obtained were adequate to demonstrate the testing technique, accuracy varied between the different test conditions.[9] The spring and lubrication systems used in the Magnus rotor test represents a considerable improvement from that used in the initial test with the smooth cylinder, in that a complete 360 deg circumferential survey can be obtained during a single test.

The Magnus rotor is a aerodynamic configuration with an irregular external surface as opposed to the smooth surfaced cylinder tested previously. This requires that surface pressures be measured at specific locations relative to the model external features. A total of 8 vent holes are located in the

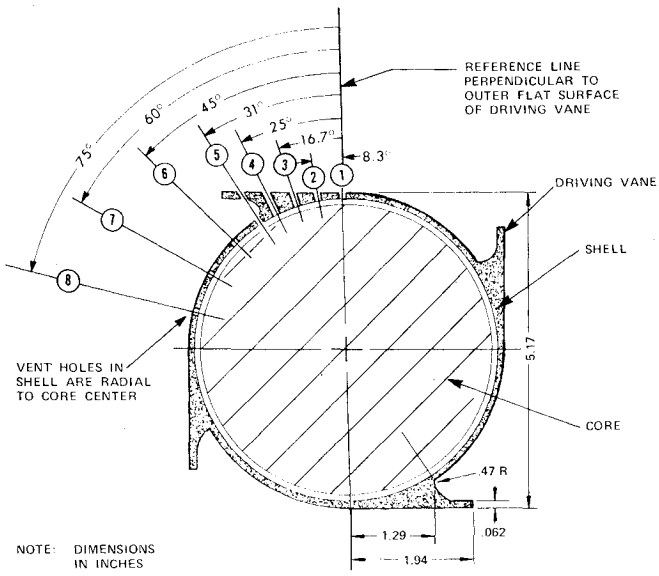

Fig. 3 Vent hole locations.

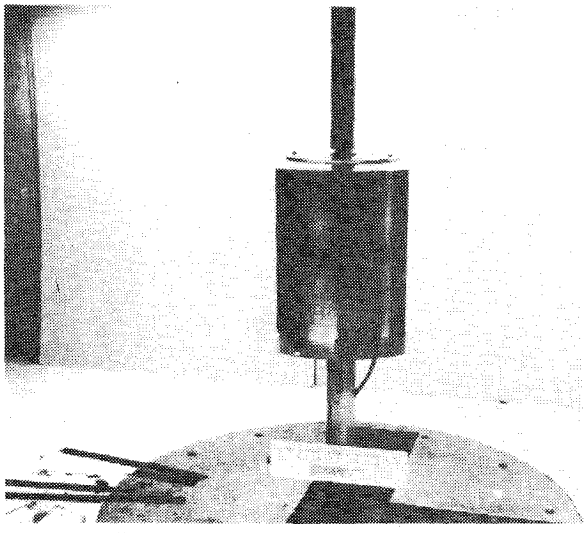

Fig. 4 Model mounted in wind tunnel.

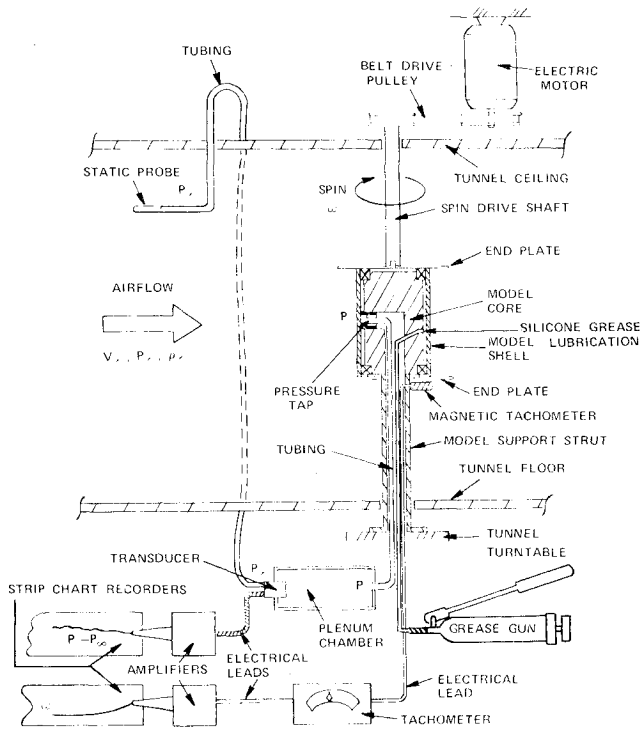

Fig. 5 Model installation and instrumentation arrangement.

model shell as defined in Fig. 3. Because of the 90 deg rotational symmetry, the model only requires vent holes over a single quadrant. The lengths of vent holes 8, 7, 6, and 1 are equal to the model shell thickness of 0.125 in. Vent holes 5, 4, 3, and 2 have to pass through the thickness of the driving vane resulting in longer vent hole paths; the longest being tap 5 with a total length of 0.625 in.

Instrumentation Arrangement and Test Procedure

The wind tunnel tests were conducted in the ARRADCOM, Weapons Systems Concepts Team (WSCT) 28 × 40 in. open circuit, continuous flow subsonic wind tunnel. Figure 4 shows the model installed in the tunnel test section.

The model was mounted in the tunnel with the longitudinal (i.e., spin axis) in a vertical attitude and normal to the freestream velocity. The mounting and instrumentation arrangment is shown in Fig. 5. The model was spun at 2050 rpm by means of an electric motor providing the desired 0.46 steady state tip speed ratio for the tunnel velocity of 100.5 fps. The steady state tip speed ratio for the autorotating model had been determined from separate wind tunnel tests using a free spinning Magnus rotor model. Although the model shell contained eight vent holes, only one hole was open for a specific test run; the others being plugged closed with soft solder.

The testing procedure was to first establish the air flow in the tunnel test section at the desired velocity. The spin motor then rapidly brought the model shell up to the steady state spin rate condition. The model core was rotated to a particular angular position by means of the tunnel turntable. Between 30 and 60 s were required to allow the pressure reading to stabilize and be recorded. The core was then rotated to the next position while the model was spinning. This procedure was repeated at 10 deg increments over the entire circumference of the model surface. The vent hole was then closed off, another opened up and the test sequence repeated until a circumferential pressure distribution was obtained for each vent hole location. Figure 6 represents typical test data obtained for vent holes 5 and 8. The transducer measured the surface pressures relative to the freestream static pressure. The data were reduced to coefficient form as defined in Fig. 7 and presented graphically, where the magnitude of the pressure coefficient at each circumferential location is denoted by a proportional length arrow emanating radially from an outline of the model. The direction of each arrow indicates whether the pressure at that point is greater than the freestream static pressure (i.e., directed toward the surface) or less than the freestream static pressure (i.e., directed away from the surface).

Data Reduction Technique

Figure 8 includes the reduced pressure data plots for all of the vent hole locations. These data indicate the pressure acting at that particular location on the surface of the model during a complete 360-deg rotation of the model relative to the freestream direction. Data in this form provide a detailed insight into the fluid mechanics and the source of the resultant aerodynamic forces. Note the large negative pressures present on the surface at the forward tip of the driving vane (vent hole 5) during the retreating phase of its motion.

The data in Fig. 8 provide the basis for determining the pressure distribution acting over the entire surface of the model at a particular instant of time. Because of the 90-deg

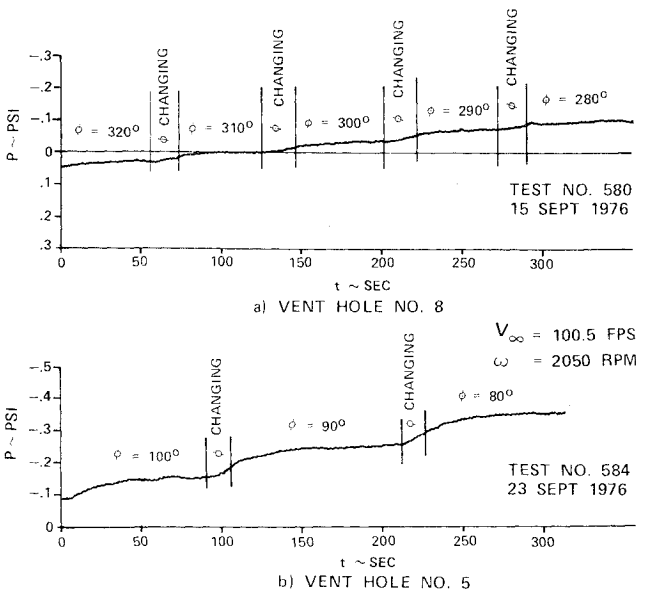

Fig. 6 Representative surface pressure measurements.

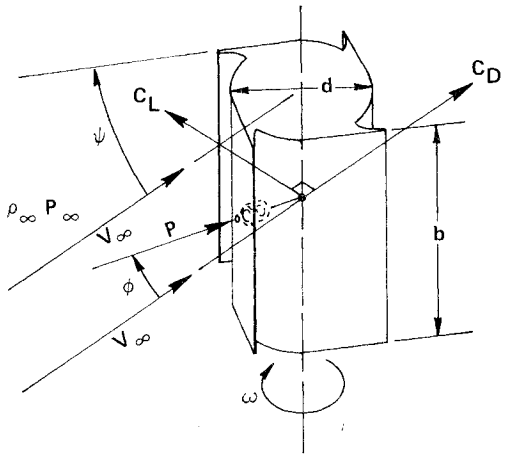

Fig. 7 Definition of data terms.

symmetry of the four vane model, a particular vent hole is located at four different circumferential positions relative to the freestream vector at a given instant of time (or a corresponding rotational attitude of the model). For example, Fig. 9a shows the basic circumferential pressure distribution for vent hole 8. From these data, the four pressure values at this vent hole location are indicated in Figs. 9b and 9c for model rotational attitudes of 0 and 45 deg, respectively. The time increment occurring between these rotational attitudes can be determined from the spin rate of the model to be 3.6 ms. Using the basic data plot for a given vent hole location, the pressure at any rotational attitude and corresponding time can be determined.

For convenience and clarity the basic pressure plots are all presented in terms of radially directed pressure coefficients. However, vent holes located on model surface features not normal to the radial direction such as on the driving vanes, must have the pressure data reoriented normal to the surface feature as illustrated in Fig. 10.

Following this procedure with the data for all the vent holes, the complete surface pressure distribution acting over the spinning Magnus rotor can be determined.

Test Results

Figure 11 shows the pressure distribution acting on the spinning Magnus rotor model over a quarter revolution at 11.25 deg increments. Note that for the 2050 rpm spin rate of

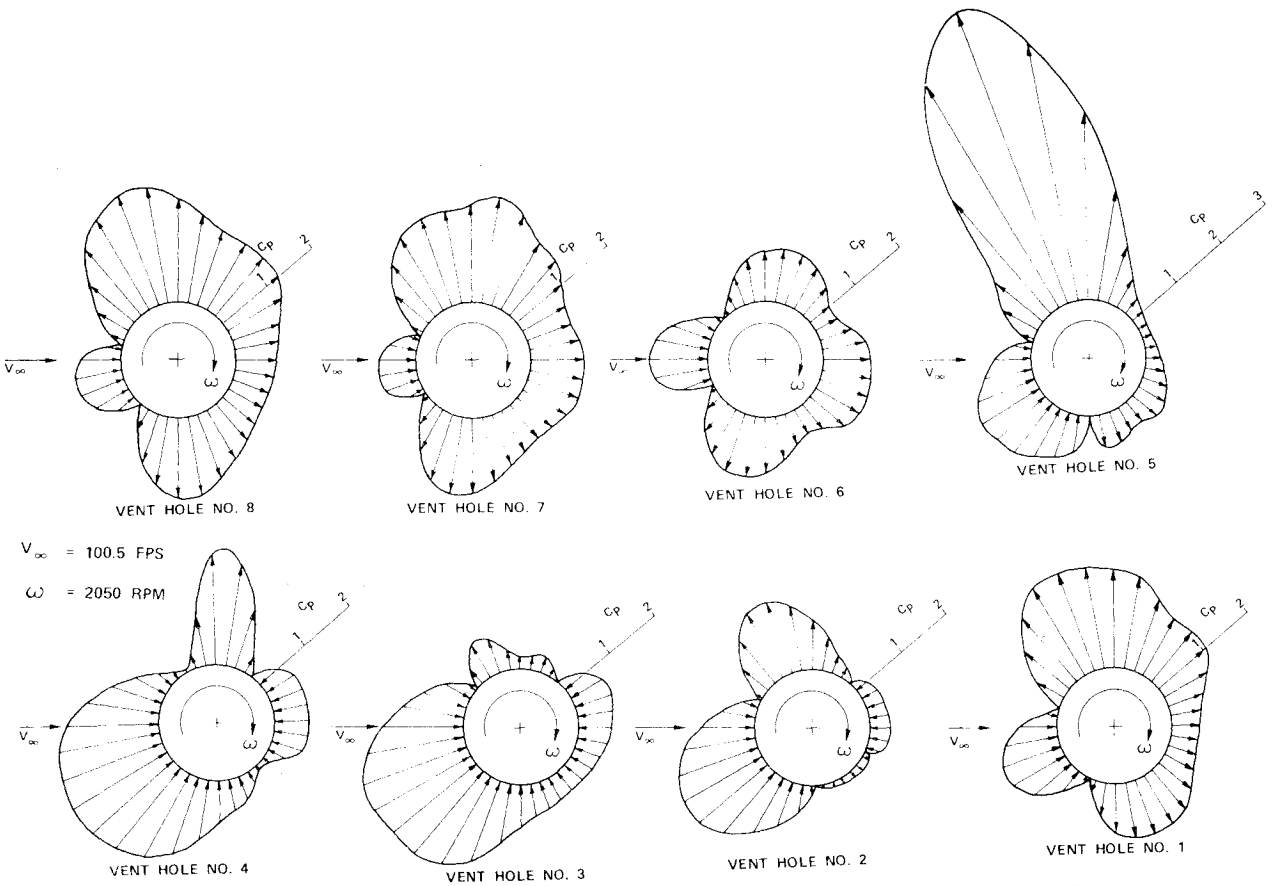

Fig. 8 Surface pressure at various vent hole locations during one revolution of the model shell.

the model, this corresponds to the pressure distribution at 1-ms intervals and is repeated four times during a complete 360-deg revolution. Because of the nature of the testing method, once the basic data plots are obtained, pressure distributions can be determined at any time increment.

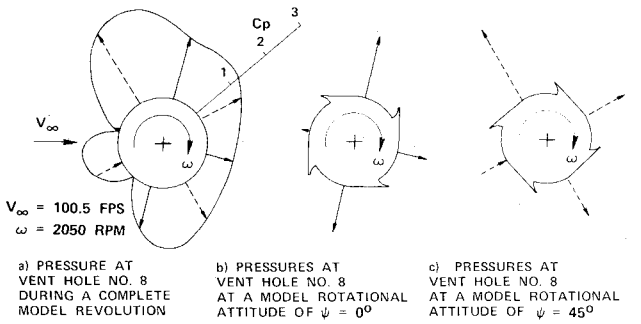

Fig. 9 Determination of surface pressures at vent hole #8 for two-model rotational attitudes.

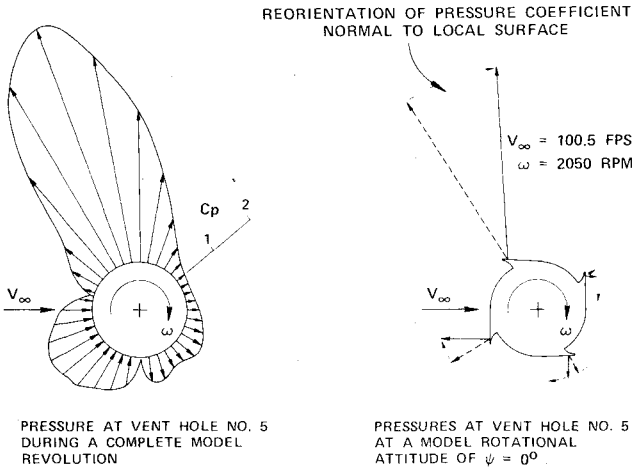

Fig. 10 Determination of surface pressure at vent hole #5 (vane surface) for a particular model rotational attitude.

driving vanes. Since there were no vent holes located on the undersides of the vanes, this effect is not included in the integrated pressure data, resulting in both a lower drag and lower lift.

Data Analysis

In order to better interpret the surface pressure data, a series of flow visualization wind tunnel tests were conducted in a special smoke flow facility at the University of Notre Dame. A 4-in. diam free-spinning model identical in external configuration to the pressure model was used in these tests. High speed film records were made of the flow over the spinning model at several test conditions.

The resultant lift and drag coefficients for each pressure distribution shown in Fig. 11 were computed by integrating the pressure distribution over the surface. These values are presented as a function of model rotational attitude and time in Fig. 12. Note that the lift and drag are sinusoidal and out of phase, with maximum and minimum lift occurring at model rotational attitudes ψ of 35 and 75 deg, respectively, and maximum and minimum drag occurring at 50 and 10 deg, respectively.

Prior to the pressure measurement tests, a static force wind tunnel test was conducted to determine the aerodynamic force and spin characteristics of the cylindrical Magnus rotor configuration. These tests were conducted with the same model and in the same facility as the pressure tests. Removal of the internal pressure tap assembly and the motor drive shaft allowed the model shell to spin freely under the action of the air flow. The model strut was attached to a pyramidal strain gage balance located beneath the test section floor. The vertical support strut was enclosed in a streamlined wind shield to reduce tare effects. Lift, drag, and steady-state spin rate were measured at various freestream velocities. The steady-state tip speed ratio used in the pressure tests was determined from these static force tests. The average values for both the lift and drag as determined from the pressure data are shown in Fig. 13 along with the values directly measured during the static force wind tunnel tests. The differences between the two sources of data are probably due to the effect of the pressure acting on the underside of the

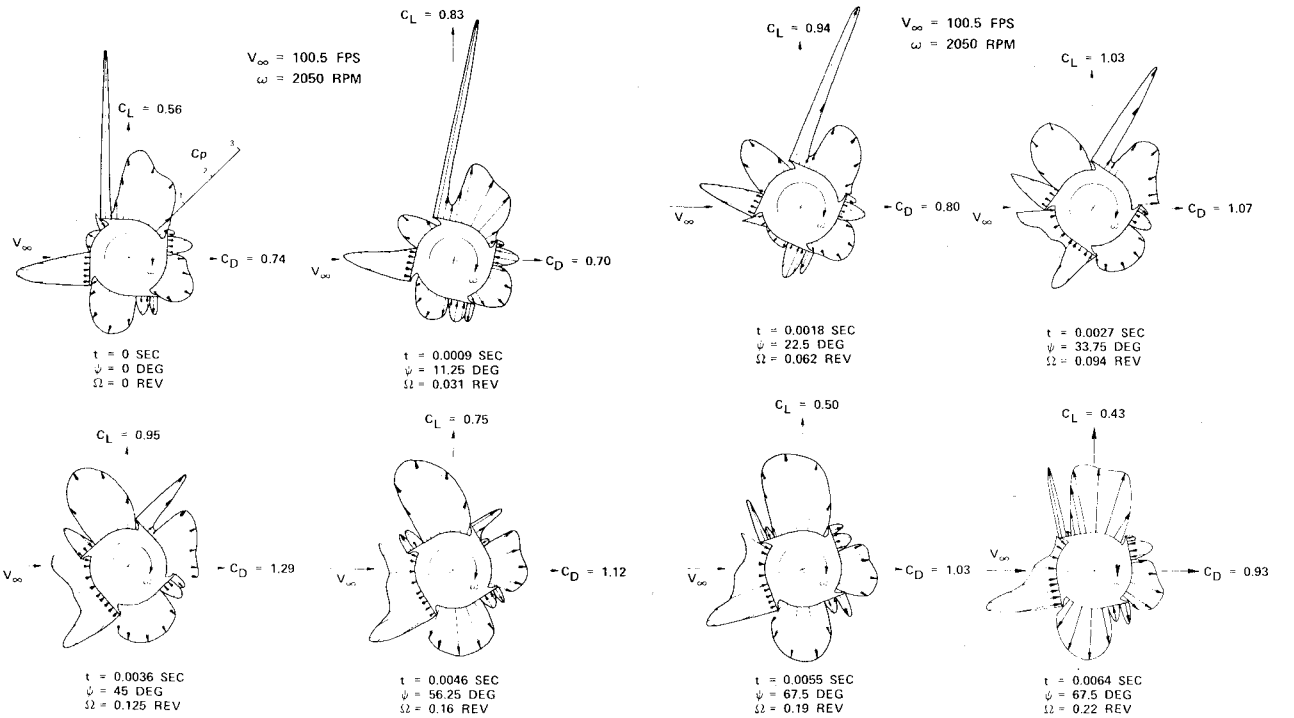

Fig. 11 Surface pressure distribution on spinning Magnus rotor at 1- ms intervals.

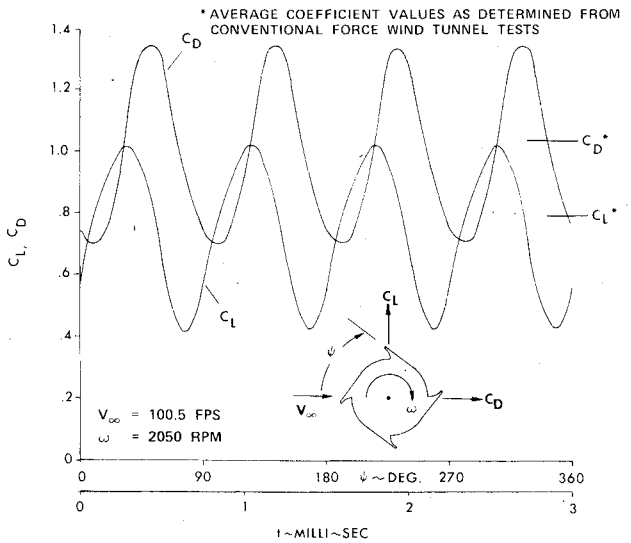

Fig. 12 Lift and drag coefficient as a function of time for the spinning Magnus rotor.

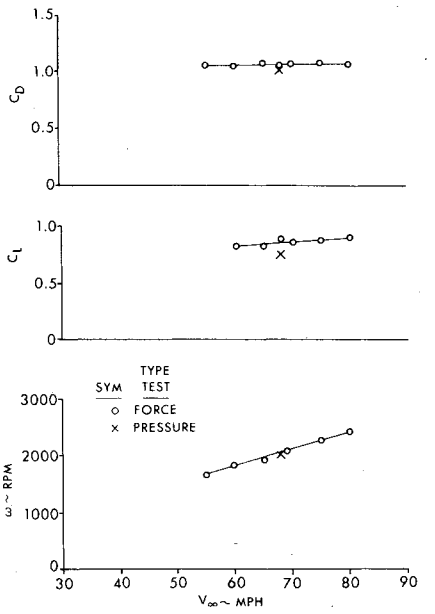

Fig. 13 Static aerodynamic characteristics of Magnus rotor at steady-state spin.

Figure 14 contains selected film frames at the same model rotational attitudes as the pressure data of Fig. 11. These photographs illustrate the unsteady separated flowfield and, in particular, the strong vortex shed off the retreating (upper) driving vane.

The film frames for model rotational attitudes ψ of 0, 22.5, 45, and 67.5 deg were used to construct line drawings of the flowfield streamlines at these conditions. Note that the 90 deg angle would be identical to the 0 deg case. Figure 15 shows the flowfields for these cases superimposed on the pressure distribution measured for the same conditions. This provides a simultaneous presentation of the flowfield, aerodynamic pressure distribution, and resultant aerodynamic forces for

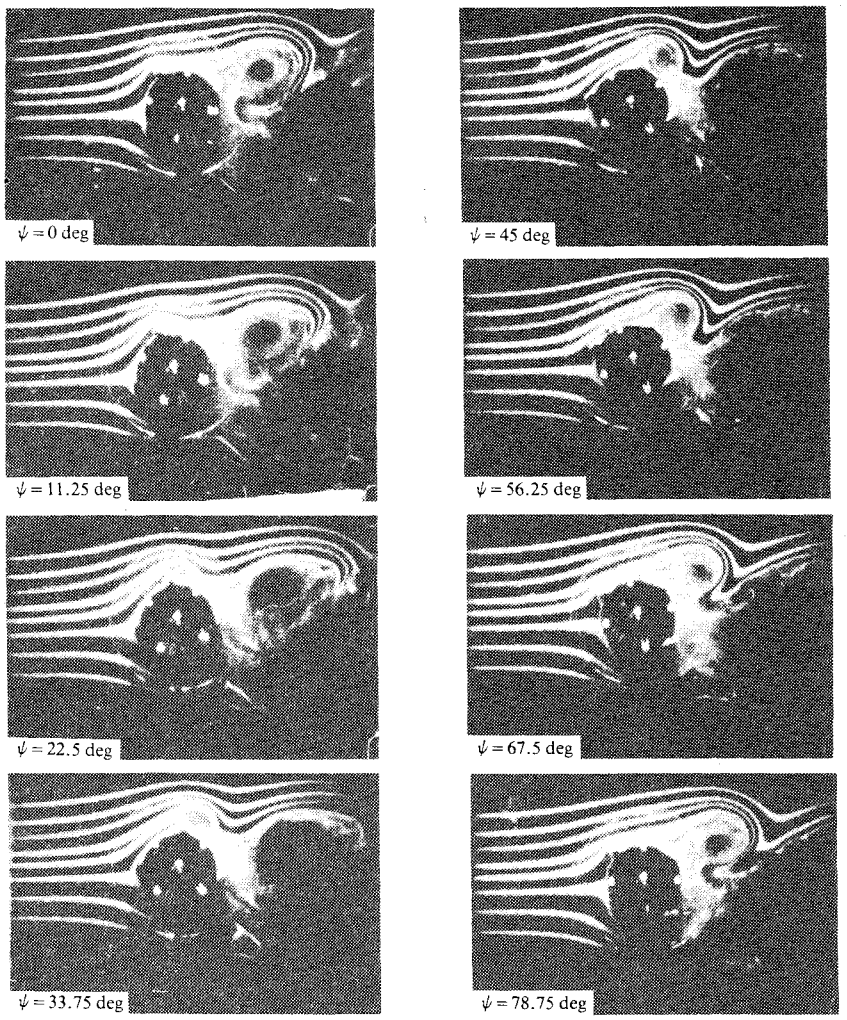

Fig. 14 Flowfield over spinning Magnus rotor model (V_∞ = 30 fps, ω = 790 rpm, $\hat{\omega}$ = 0.46).

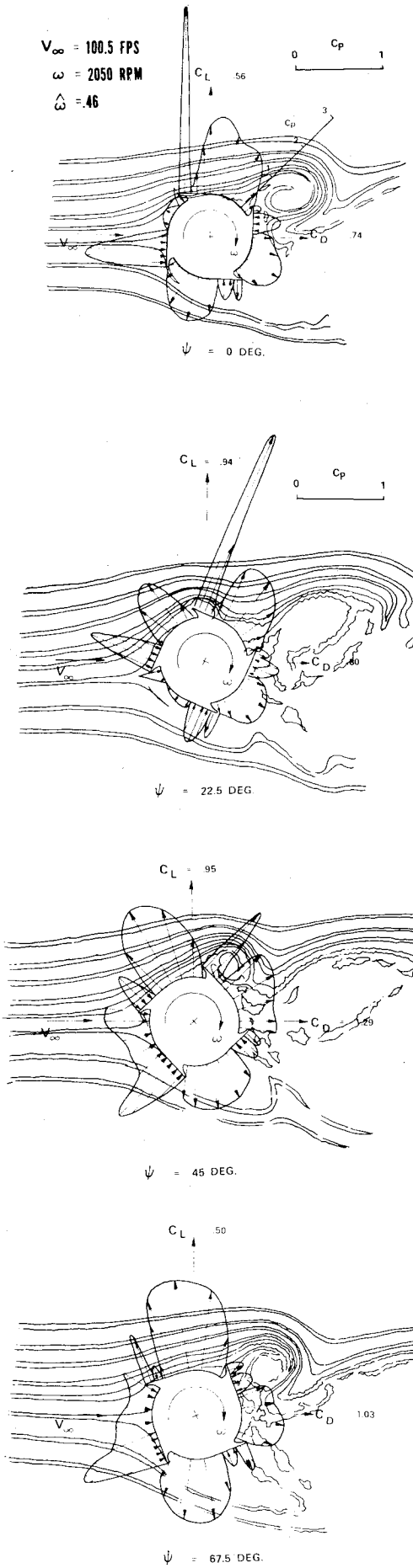

Fig. 15 Flowfield, surface pressure distribution, and aerodynamic forces on spinning Magnus rotor at various rotational attitudes.

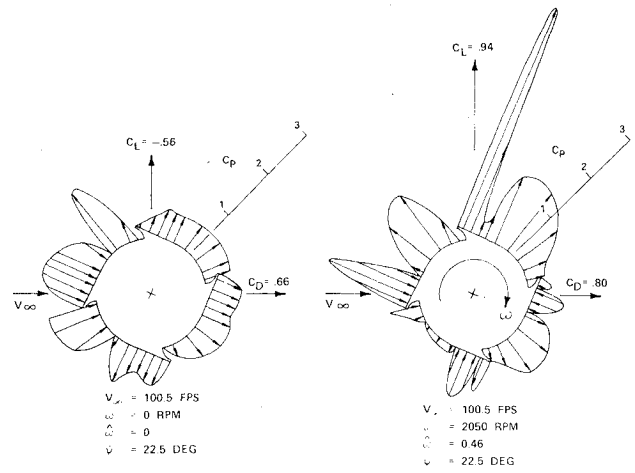

Fig. 16 Effect of spin on Magnus rotor surface pressure distribution.

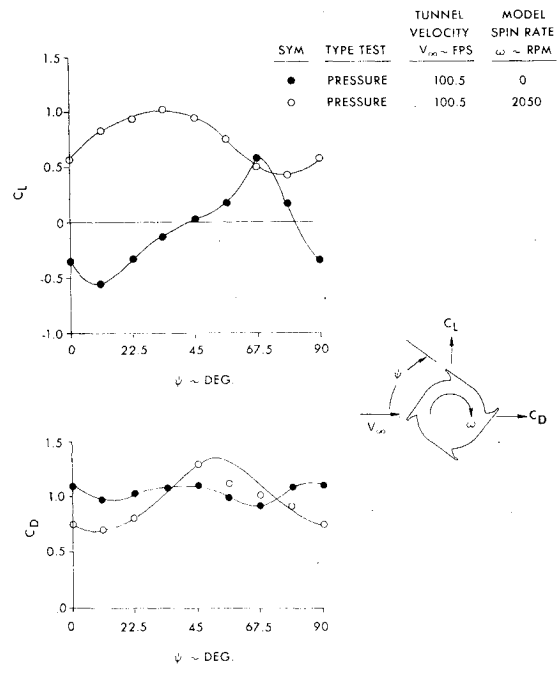

Fig. 17 Effect of spin on Magnus rotor lift and drag at various model rotational attitudes.

the spinning Magnus rotor at a given instant of time. Note how the vortex created by the sharp leading edge of the retreating driving vane produces a local high velocity flow and corresponding low pressure over the forward portion of the vane. The swirling motion of the vortex results in a local air flow further back on the vane that is essentially normal to the vane surface, resulting in a stagnation-like flow situation, a corresponding reduction in the negative pressure, and in some cases, actually producing a positive pressure region.

The flow, although unsteady, is periodic with model rotation. It is this latter factor that allows this pressure measuring method, which essentially uses steady-state instrumentation to measure an unsteady flow situation.

Effect of Spin

A series of pressure measurements were also made on the non-spinning Magnus rotor. For these tests the shell was positioned relative to the core such that a particular vent hole was located directly over the pressure tap. With the shell locked to the core by means of a set screw, the non spinning model was then incrementally rotated through 360 deg with

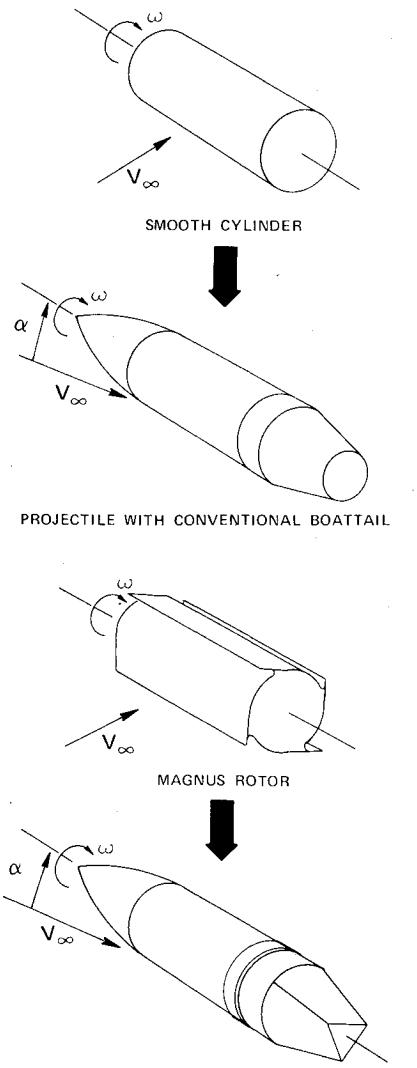

Fig. 18 Future applications of pressure measuring method.

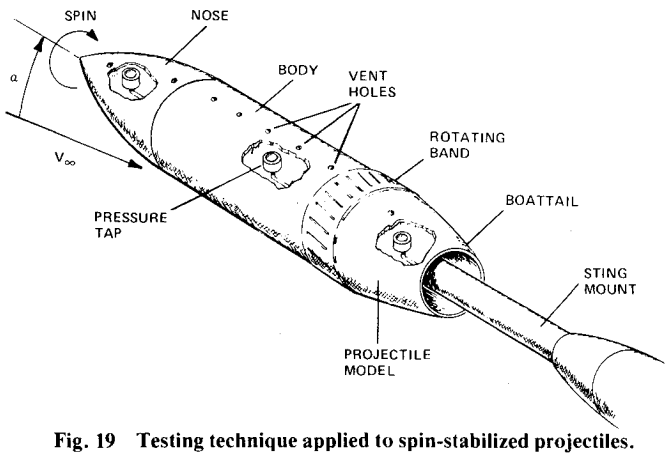

Fig. 19 Testing technique applied to spin-stabilized projectiles.

pressure data being measured every 10 deg. The resulting data were reduced as in the spinning case, resulting in the pressure distribution acting over the non-spinning Magnus rotor.

Figure 16 shows the resultant pressure distribution on the spinning and non-spinning model at a model orientation of 22.5 deg. Note that at this attitude, the non-spinning Magnus rotor generates a negative lift force. For the spinning case, the rotating vane leading edge produces and sheds a vortex during each revolution, influencing the pressure distribution over the entire model surface and resulting in a net positive lift.

Figure 17 shows the variation in lift coefficient as a function of rotational attitude for both the spinning and non-spinning Magnus rotor. For the non-spinning case, the lift assumes both positive and negative values depending on model attitude, whereas the spinning model experiences a net positive lift at all attitudes. The corresponding drag coefficient characteristics are also shown in Fig. 17. In this case, the spinning model drag coefficient shows more variation with model attitude, but its net result is similar to the non-spinning case.

The difference between the spinning and non-spinning data at model attitude angles around 50 deg is, as before, probably due to the effect of the pressure acting on the underside of the driving vane.

Future Applications

As the previous tests with the smooth cylinder should allow extension of the testing method to a variety of spinning models having smooth external shapes, so the Magnus rotor results allow the method to be used with spinning models having irregular external configurations as illustrated in Fig. 18. This could even include spin stabilized projectiles having external surface features such as rotating bands and unconventional boattails.[10] However, this testing methodology is applicable only for steady flow situations or "special" unsteady cases where the flowfield is a function of the rotational attitude of the spinning body.

Multiple pressure taps could be incorporated into a wind tunnel model at several locations along its length as shown in Fig. 19, providing the pressure distribution acting over the entire model surface. Because the pressure measuring elements are completely internal, the models could be tested at any angle of attack and in all Mach number regimes. The use of this testing method could provide new insights into a variety of spin related aerodynamic problems.

Conclusions

This study has demonstrated a new testing method by which the aerodynamic pressure distribution acting on the surface of a spinning body having irregular surface features can be measured in the wind tunnel. Integration of the resulting pressure distribution data not only provide a quantitative measure of the aerodynamic forces, but the pressure profile allows interpretation of this special case of non-steady, periodic flow. The test method should be applicable to a variety of model configurations, angles of attack, spin rates, and Mach number regimes.

References

[1] "Autorotating Magnus Rotor Aero-Design Handbook," Arnold Engineering and Development Center, AEDC-TR-75-24, July 1975.

[2] Iverson, J.D., "The Magnus Rotor as an Aerodynamic Decelerator," AIAA Paper 68-962, Sept. 1968.

[3] Miller, M.C., "A Dynamic and Aerodynamic Analysis of an Articulated Autorotor Decelerator," AIAA Paper 73-463, May 1973.

[4] Vance, W., "Vertical Axis Wind Rotors—Status and Potential," *Workshop Proceedings, Wind Energy Conversion Systems*, National Science Foundation, NSF/RA/W-73-006, June 11-13, 1973.

[5] Lugt, H.J., "Autorotation of Plates," David W. Taylor Research and Development Command Rept., DTNSRDC-78/058, Aug. 1978.

[6] Zipfel, P.H., "On Flight Dynamics of Magnus Rotors," Tech. Rept. 117, Munitions Development Division, Ft. Detrick, Md., Nov. 1970.

[7] Miller, M.C., "A Technique to Measure the Pressure Distribution Acting on the Surface of a Spinning Body in a Wind Tunnel," Edgewood Arsenal Tech. Rept. ED-TR-76070, Sept. 1976.

[8] Miller, M.C., "Surface Pressure Measurements on a Spinning Wind Tunnel Model," *AIAA Journal*, Vol. 14, Dec. 1976, p. 1669.

[9] Miller, M.C., "Method to Experimentally Determine the Aerodynamic Pressure Distribution on Spinning Bodies," *Tenth Army Science Conference Proceedings*, AD-A056468, Vol. 11, June 20-22, 1978, pp. 433-447.

[10] Platou, A.S., "Improving the Flight Performance of Projectiles," Ballistic Research Laboratory, Aberdeen Proving Ground, Md., Rept. ARBRL-TR-02165, May 1979.